

# DEM Modelling on the Interface Behavior of Geogrid-stabilized Sub-ballast

Trung Ngo, Ph.D., M.ASCE<sup>1</sup>, Buddhima Indraratna, Ph.D., F.ASCE,<sup>2</sup> and  
Cholachat Rujikiatkamjorn, Ph.D., M.ASCE<sup>3</sup>

<sup>1</sup>Senior lecturer, Transport Research Centre, School of Civil and Environmental Engineering, University of Technology Sydney, 15 Broadway, Ultimo NSW 2007, Australia.

E-mail: [Trung.Ngo@uts.edu.au](mailto:Trung.Ngo@uts.edu.au)

<sup>2</sup>Distinguished Professor of Civil Engineering and Director, Transport Research Centre, School of Civil and Environmental Engineering, University of Technology Sydney 15 Broadway, Ultimo, NSW 2007, Australia; Founding Director, ARC Industrial Transformation Training Centre for Advanced Technologies in Rail Track Infrastructure (ITTC-Rail), University of Wollongong, NSW 2522, Australia.

Email: [Buddhima.Indraratna@uts.edu.au](mailto:Buddhima.Indraratna@uts.edu.au)

<sup>3</sup>Professor, Transport Research Centre, School of Civil and Environmental Engineering, University of Technology Sydney, 15 Broadway, Ultimo NSW 2007, Australia. Program Coordinator, ARC ITTC-Rail, University of Wollongong, NSW 2522, Australia.

Email: [Cholachat.Rujikiatkamjorn@uts.edu.au](mailto:Cholachat.Rujikiatkamjorn@uts.edu.au)

## ABSTRACT

This paper presents a study on the interface behavior of geogrids and sub-ballast (capping) using a series of large-scale direct shear tests and discrete element modelling (DEM). Direct shear tests were carried out on sub-ballast with and without geogrid inclusions. The laboratory test data show that the interface shear strength is governed by normal stress and types of geogrid. The three-dimensional discrete element method (DEM) was used to study the interface shear behavior of the sub-ballast subjected to direct shearing loads. Irregular-shaped particles of capping aggregates were modelled by clumping of many balls together in appropriate sizes and positions. Different types of geogrids were modelled by bonding small spheres together to form the desired grid geometry and apertures. The DEM model was then used to investigate the evolutions of contact force distributions and fabric anisotropy during the shear tests and the role of geogrid in micro-mechanical perspective.

## INTRODUCTION

Ballasted rail tracks have gained a competitive edge over other modes of transportation systems in terms of performance, better ride quality, higher safety, lower cost of construction and relatively acceptable speed and efficiency of services (Selig and Waters 1994). Despite concerted efforts by

rail organizations to improve performance, excessive degradation and deformation of ballasted tracks continue to impart substantial maintenance costs (Tutumluer et al. 2013, Li et al. 2015). Under cyclic loading induced by passing trains, the granular aggregates gradually degrade and begin to lose their shear strength and drainage capacity. As a result, ballast and sub-ballast (capping) layers often undergo excessive lateral spreading, leading to substantial differential track settlements, causing regular costly maintenance. Also, the presence of soft estuarine clay deposits along the coastal belt of Australia pose serious concerns on track stability. Considering significant demand for urban transportation as well as substantial urban growth, the construction of new tracks, maintenance and modernization of existing tracks become more challenging (Priest et al. 2010, Biabani et al. 2016, Jiang et al. 2016). It is well recommended that innovative solutions need to be pursued to improve ballasted rail track substructure, which can help to increase passenger comfort and maintain the railway as the most economical and safest mode of transportation in Australia (Indraratna and Ngo 2018). In the view of above, reinforcing a capping layer is one of the economic and imperative alternatives for stabilizing the track substructure.

Unlike conventional rigid reinforcements such as steels or timbers, flexible geosynthetics have shown a promising approach for improving the performance of granular media (ballast and sub-ballast) placed over weak and soft subgrade (Bathurst and Raymond 1987, Bathurst et al. 2009, Tutumluer et al. 2012). Different types of planar geogrids have been successfully employed to reinforce track sub-structures. Having placed inside the granular layer, a geogrid acts presumably as a non-horizontal displacement boundary that confines the surrounding particles via the interlocking and frictional resistance between itself and the ballast aggregates, and thus restrains deformation of ballasted track substructure (Brown et al. 2007, Han and Bhandari 2009, Biabani et al. 2016, Ngo et al. 2017, Indraratna et al. 2019, Qian et al. (2018)). These studies have proven that the use of planar geogrids was a practical approach to reducing the settlements and enhancing track stability. It is also noted that railway organizations often concern using geogrids to confine the ballast layer because of practical difficulties encountered with using the tamping machine during track maintenance. Based on laboratory test results, Biabani et al. (2016) showed that reinforcing an underlying capping material with a layer of geogrid is a feasible solution.

This paper presents a study of the interface behavior of reinforcing geogrid and sub-ballast using a series of large-scale direct shear tests and discrete element modelling (DEM). Direct shear tests were conducted for sub-ballast with and without geosynthetics inclusions under varying normal stresses. DEM simulations were carried out to investigate the behavior of reinforced granular media under shearing load and further investigate the micro-mechanical responses of geogrid-reinforced capping assemblies.

## **LABORATORY TESTS**

Sub-ballast material used in this study was crushed basalt collected from a quarry near Wollongong, NSW, Australia. A particle size distribution (PSD) of the sub-ballast tested in the laboratory ( $D_{max} = 19$  mm,  $D_{min} = 0.75$  mm,  $C_c = 1.3$ ,  $C_u = 16.3$ ) in comparison with the others

were used in the railway industry are presented in Figure 1. Three types of geogrids having varied geometry and apertures (biaxial geogrids, BG1, BG2 and triaxial geogrid, TG1) were used in the laboratory (Figure 2a) to examine the effects of opening aperture and geometry of geogrids on the interface shear strength. A large-scale direct shear testing apparatus consisting of a 300mm × 300mm square steel box, 200 mm high, divided horizontally into two equal halves, was used for the laboratory tests. All instruments were calibrated before connecting to an electronic data logger (DT800) and a host computer to precisely record shearing loads, vertical and lateral displacements, load cells and strains induced in the geogrids at predetermined time intervals (Figure 2b).

Capping materials were placed in the bottom half of the shear box and compacted to achieve a unit weight of approximately  $\gamma_d = 18.5 \text{ kN/m}^3$ . A sheet of geogrid was then placed at the interface of upper and lower boxes and was then securely clamped to the shear. The upper half of the shear box was then filled with capping aggregates and compacted. Laboratory tests with and without the inclusion of geogrids were conducted at a relatively low normal stress of varying from  $\sigma_n = 6.7 \text{ kPa}$  to 45 kPa to simulate the low confinement in actual tracks and were sheared to a shear strain of  $\varepsilon_s = 10\%$ . During the tests, shear forces, vertical and horizontal strains were recorded at every 1mm of shear displacement. The laboratory test data show that the interface shear strength was governed by normal stress and types of geosynthetics tested (Biabani and Indraratna 2015). Test data is used in this paper to calibrate and validate the DEM model as presented in the following sessions.

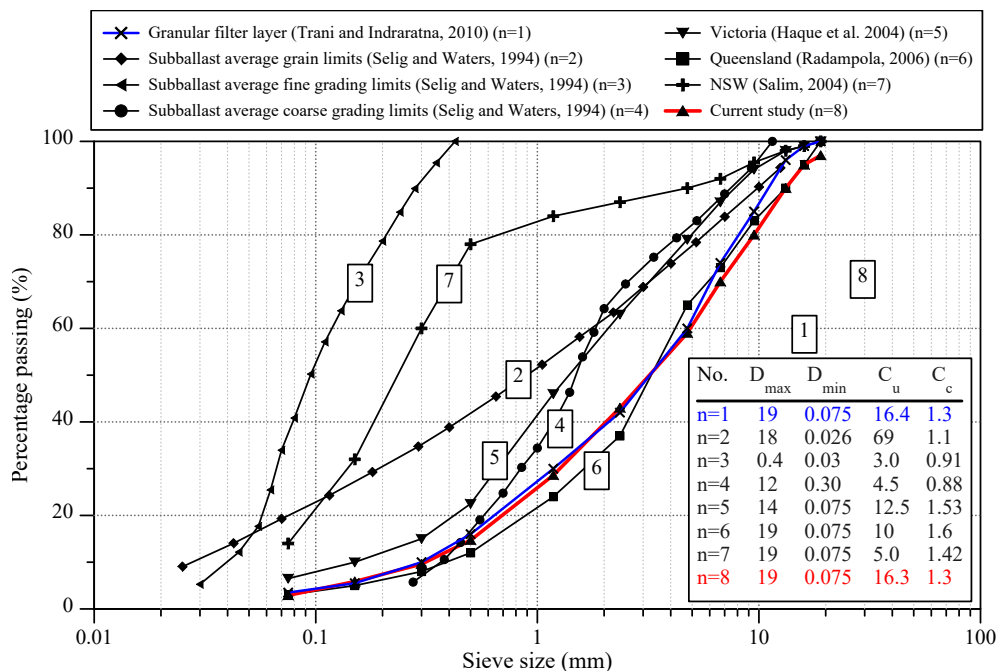


**Figure 1. Grain size characteristics of the capping material tested in the laboratory in comparison with other materials (modified after Ngo et al. 2017 - with permission from Springer)**

## DISCRETE ELEMENT MODELING (DEM)

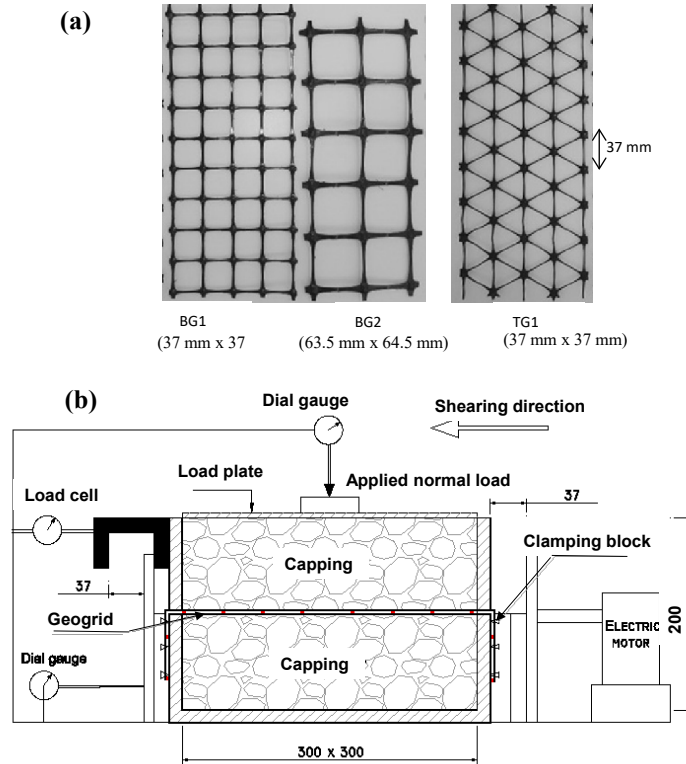
Numerical modelling is one of the cost-effective tools that has been widely developed with different degrees of complexity and accuracy to investigate the dynamic performance of track substructure layers during the passage of moving trains (Tang et al. 2019, Jing et al. 2020). The Discrete element method (DEM) introduced by Cundall and Strack (1979) has been used to investigate the micro-mechanical behavior of granular materials. The DEM enables to insightfully explore the contact force distributions developed between particles, evolutions of fabric anisotropy where the irregularly-shaped particles and breakage of particles can be accurately captured (Lobo-Guerrero and Vallejo 2006, O'Sullivan and Cui 2009, Ngo et al. 2021, Lu and McDowell 2010, Ngo et al. 2017, Zhang et al. 2017, Tutumluer et al. 2009, Feng et al. 2019, among others).

In the current DEM analysis, three types of geogrids (BG1, BG2 and TG1) that are identical to those tested in the laboratory were simulated, as shown in Figure 3. The geogrids were simulated by spheres of different sizes to simulate actual geometry, where the bigger balls were used to model the geogrid junctions and the smaller balls at the centre of the ribs. Spheres were connected by parallel bonds corresponding to geogrid's tensile strength that can be determined by tensile tests. Each bond represents the load-displacement responses of a finite-sized piece of cementitious material deposited between two spheres in contact and transmits both forces and moment (Itasca 2018). Capping aggregates were scanned through a 3D particle imaging built-in with a laser scanner to construct realistic polyhedral discrete particles. A set of subroutines was programmed to discretize ballast particles in DEM by clustering spheres with specified sizes and locations to fill up the polygonal mesh. Determining the model parameters for geogrids and capping can be complex considering a large number of required parameters, i.e., stiffness ( $k_n$ ,  $k_s$ ), friction coefficient ( $f$ ) and other parameters. In this study, micro-mechanical parameters were determined by back-calculation of shear stress-strain responses with those measured from laboratory tests. A set of micromechanical parameters adopted for modelling the geogrid and capping materials is given in Table 1. DEM model to simulate direct shear test for geogrid-reinforced sub-ballast are shown in Figure 4.

## RESULTS AND DISCUSSION

Figure 5 compares the shear stress ratio versus shear strain obtained by DEM with those measured in the laboratory reported by Biabani and Indraratna (2015). Generally, the predicted curves agree well with the experimental data. Triax geogrid (TG1) exhibits the highest ratio of  $\frac{\tau}{\sigma_n}$ , while the biaxial geogrid (BG2) shows the lowest shear stress ratio and highest dilation rate. The sub-ballast assembly reinforced by the Triax experiences the lowest volumetric dilation. This is believed that the Triax geogrid has symmetric geometry (triangular apertures) that distributes stress more uniformly across the geogrid and that provides a better interlocking mechanism with grains. The Triax geogrid's improved performance may also be attributed to the isotropic radial stiffness of the

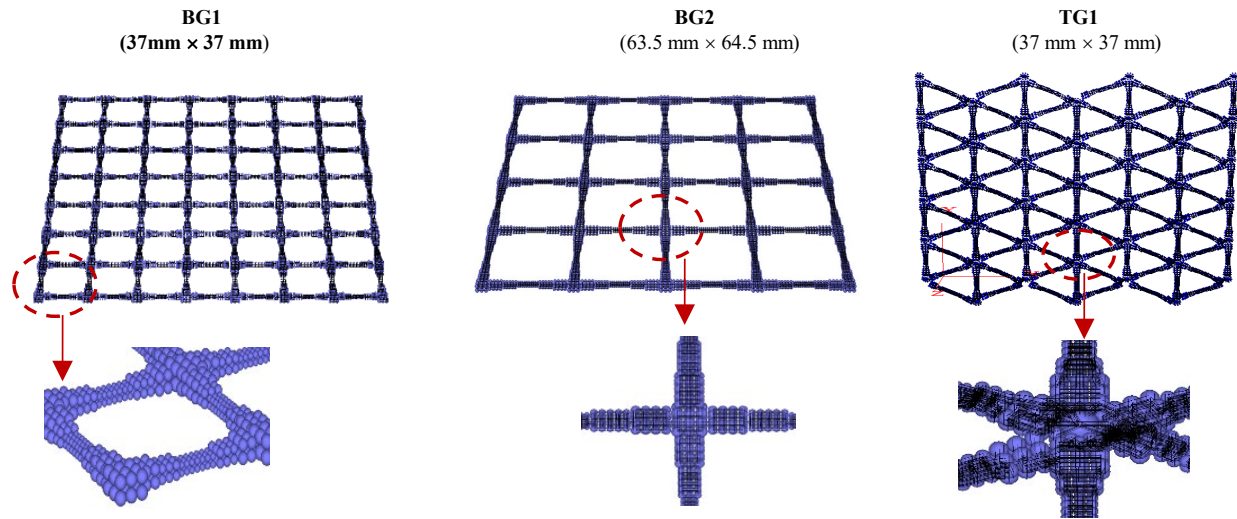
TG1 which is nearly consistent in all directions, resulting in better confinement with sub-ballast aggregates at their interfaces.



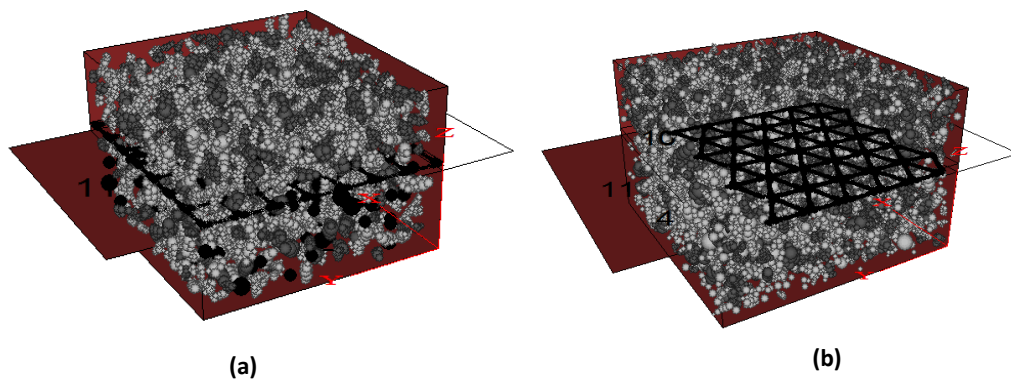
**Figure 2. Geogrid tested in the laboratory and Schematic diagram of the large-scale direct shear test set up (dimensions are in mm)**

Table 1. Micromechanical properties of geogrid adopted for DEM simulation

Material	Parameter	value
Geogrid	Particle density ( $\text{kg/m}^3$ )	800
	Contact normal stiffness, $k_n$ (N/m)	$1.77 \times 10^7$
	Contact shear stiffness, $k_s$ (N/m)	$1.77 \times 10^7$
	Contact bond normal strength, $F_n$ (kN)	75 kN
	Contact bond shear strength, $F_s$ (kN)	75 kN
	Parallel bond radius multiplier, $r_p$	0.5
	Parallel bond normal stiffness, $k_{np}$ (GPa/m)	$5.68 \times 10^5$
	Parallel bond shear stiffness, $k_{ns}$ (GPa/m)	$5.68 \times 10^5$
	Parallel bond normal strength, $\sigma_{np}$ (GPa)	$4.56 \times 10^5$
Sub-ballast (Capping)	Particle density ( $\text{kg/m}^3$ )	2100
	Inter-particle coefficient of friction, $\mu$	0.69
	Contact normal stiffness, $k_n$ (N/m)	$4.82 \times 10^8$
	Contact shear stiffness, $k_s$ (N/m)	$2.41 \times 10^8$
	Contact normal stiffness of wall-particle, $k_{n-wall}$ (N/m)	$3.25 \times 10^9$
	Shear stiffness of wall of wall-particle, $k_{s-wall}$ (Nm)	$3.25 \times 10^9$



**Figure 3. Modelling different types of geogrids in DEM**



**Figure 4. DEM modelling of large-scale direct shear test for sub-ballast: (a) with the inclusion of biaxial geogrid (BG1); and (b) with triaxial geogrid (TG1)**

Figure 6 presents the variations of contact forces with the depth of the shear box for capping aggregates (with and without geogrid) predicted at a shear strain of  $\varepsilon_s = 5\%$ ,  $\sigma_n = 6.7$  kPa. It is clearly measured that the sub-ballast reinforced by the Triax geogrid (TG1) has the highest mobilized contact forces at the interface (i.e. approximately 71N for TG1 compared to 53N and 39 N for BG1 and BG2, respectively), while the unreinforced sub-ballast provides the lowest mobilized contact forces compared to those for the reinforced specimens. A confinement zone could be found in a depth of around 50 mm from the geogrid-capping interfaces, where the inclusion of geogrid led to a significant increase in developed contact forces.

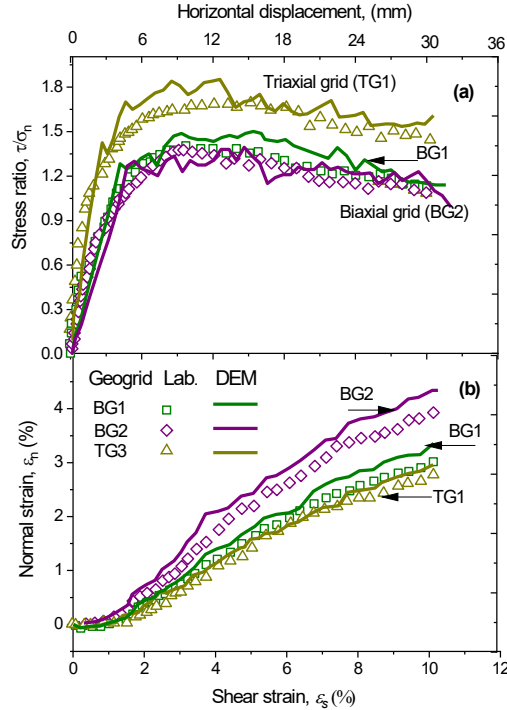


**Figure 5. Comparisons between DEM simulation and laboratory test results under  $\sigma_n = 6.7$  kPa: (a) shear stress ratio versus shear strain, (b) normal strain versus shear strain (modified after Ngo et al. 2017 - with permission from Springer)**

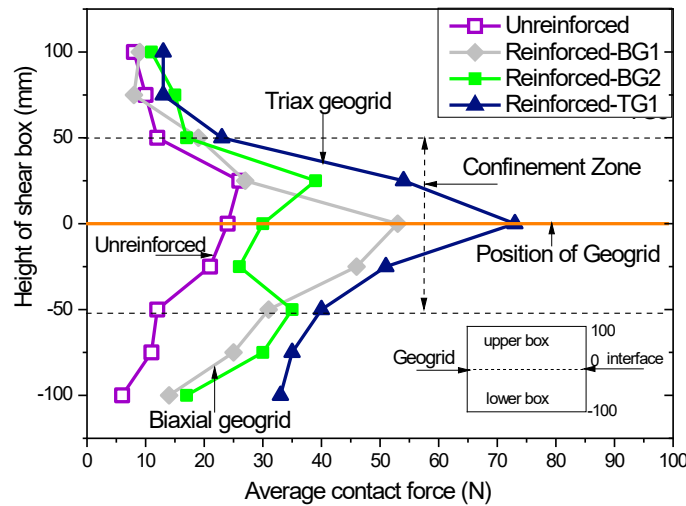
Subjected to loading, sub-ballast grains induce changes in the contact forces and subsequently changes the number of load-carrying contacts and their orientations. A fabric tensor is often used as an index to capture the packing structure of granular materials where the stress-strain responses can be expressed as force and fabric parameters (i.e. stress-force-fabric relationship). Contact forces are characterized by the probability density distribution of inter-particle contact orientation  $\bar{E}(\Omega)$  proposed by Ouadfel and Rothenburg (2001) as:

$$\bar{E}(\Omega) = \frac{1}{4\pi} [1 + F_{ij}n_i n_j] \quad (1)$$

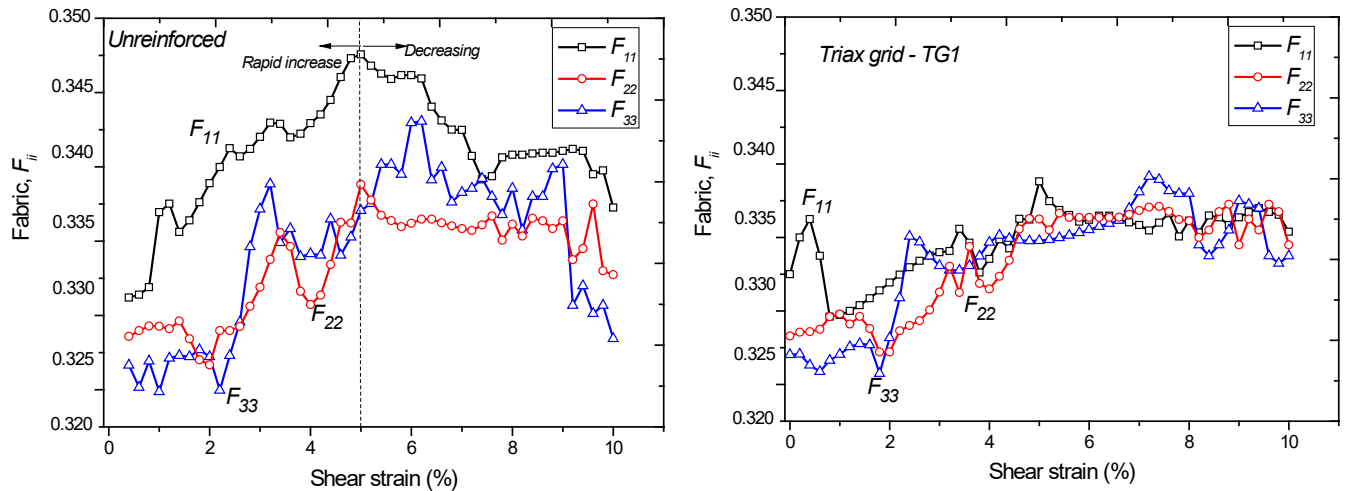
where,  $F_{ij} = \frac{1}{N_c} \sum_{k=1}^{N_c} n_i^k n_j^k$  : second order fabric tensor that represents the distribution of contact orientation. Note that  $F_{ij}$  is symmetrical (i.e.  $F_{ij} = F_{ji}$ ) with the three principal values  $F_{11}, F_{22}, F_{33}$  where their sum is unity;  $n_i^k$ : unit vector that represents the orientation of the  $k$  contact.

Figure 7 shows the evolution of fabric tensor components,  $F_{11}, F_{22}$ , and  $F_{33}$  of unreinforced and Triax geogrid-reinforced capping assemblies (TG1) during the shearing. It can be seen that the fabric varies significantly during the shearing progress. The unreinforced sub-ballast assembly exhibits much variations of fabric than reinforced assemblies, where all the fabric entries increase considerably from the beginning of shearing up to around 5% shear strain and then starts

decreasing thereafter. The reduced changes in the fabric due the inclusion of the geogrid are believed due to be the interlocking between the sub-ballast and geogrid reduces the freedom of grains to move. The increase in contact fabric at the initial stage of shearing indicates a re-arrangement and rotation of grains to support induced loads. Reinforced assemblies show relatively consistent values of fabric components,  $F_{ii}$  varying approximately from 0.325 to 0.342. The fabric component,  $F_{11}$  has the highest value for all specimens indicating that fabric contact is predominately lying in the vertical direction. It is also observed that all fabric components,  $F_{ii}$  for the Triax-reinforced sub-ballast are very close together during shearing progress while the unreinforced assembly exhibits a more significant variation.



**Figure 6. Average contact force of capping assemblies subjected to a shear strain of  $\epsilon_s = 4\%$  (modified after Ngo et al. 2017 - with permission from Springer)**



**Figure 7. Fabric evolutions of unreinforced and reinforced capping subject to shearing: (a) unreinforced (b) TG1-reinforced capping**



## CONCLUSIONS

This paper presents the results of large-scale direct shear tests on sub-ballast aggregates with and without the inclusion of different types of geogrid. The laboratory test results were used to calibrate and verify the proposed DEM models. DEM simulations for geogrids with varied shapes and opening apertures were simulated by connecting many spherical balls together. The shear stress-strain responses predicted by the DEM analysis agreed well with experimental data, showing that the current DEM model can be used to predict the interface behavior of sub-ballast aggregates reinforced by geogrids. Of the three types of geogrid tested, Triax geogrid showed the highest interface shear strength; and this was primarily due to multi-directional load distribution of the triaxial geogrid that could transfer applied loads across the geogrid and provided a better interlock with surrounding grains. The variations of mean contact forces along the depth of the shear apparatus were captured for both unreinforced/reinforced-sub-ballast specimens. The Triax geogrid-stabilized sub-ballast (TG1) provided the most significant mobilized contact forces at their interfaces. The evolution of fabric tensor components for sub-ballast assemblies with and without the inclusion of geogrids were also captured in DEM.

## ACKNOWLEDGEMENTS

The authors would like to thank the Transport Research Center (TRC) at the University of Technology Sydney for providing the support required to carry out this study. The support from the ARC-Industrial Transformation Training Centre for Advanced Technologies in Rail Track Infrastructure (IC170100006) is also acknowledged.

## REFERENCES

- Bathurst, R. J., Nernheim, A., Walters, D. L., Allen, T. M., Burgess, P. and Saunders, D. D. (2009). "Influence of reinforcement stiffness and compaction on the performance of four geosynthetic-reinforced soil walls." *Geosynthetics International*, 16(1): 43–59.
- Bathurst, R. J. and Raymond, G. P. (1987). "Geogrid reinforcement of ballasted track." *Transportation Research Record*, 1153: 8-14.
- Biabani, M. and Indraratna, B. (2015). "An evaluation of the interface behaviour of rail subballast stabilized with geogrids and geomembranes." *Geotext. Geomembr.*, 43(3): 240-249.
- Biabani, M. M., Indraratna, B. and Ngo, N. T. (2016). "Modelling of geocell-reinforced subballast subjected to cyclic loading." *Geotext. Geomembr.*, 44(4): 489-503.
- Biabani, Ngo, T. and Indraratna, B. (2016). "Performance evaluation of railway subballast stabilized with geocell based on pull-out testing." *Geotext. Geomembr.*, 44(4): 579-591.
- Brown, S. F., Kwan, J. and Thom, N. H. (2007). "Identifying the key parameters that influence geogrid reinforcement of railway ballast." *Geotext. Geomembr.*, 25(6): 326-335.
- Cundall, P. A. and Strack, O. D. L. (1979). "A discrete numerical model for granular assemblies." *Geotechnique*, 29(1): 47-65.
- Feng, S.-J., Chen, J.-N., Chen, H.-X., Liu, X., Zhao, T. and Zhou, A. (2019). "Analysis of sand – woven geotextile interface shear behavior using discrete element method (DEM)." *Can. Geotech. J.* 57(3): 433-447.

- Han, J. and Bhandari, A. (2009). Evaluation of geogrid-reinforced pile-supported embankment under cyclic loading using discrete element method. *Advances in Ground Improvement: Research to Practice in the United States and China (GSP 188)*, ASCE.
- Indraratna, B. and Ngo, T. (2018). *Ballast Railroad Design: Smart-Uow Approach*, CRC Press.
- Indraratna, B., Qi, Y., Ngo, T. N., Rujikiatkamjorn, C., Neville, T., Ferreira, F. B. and Shahkolahi, A. (2019). "Use of geogrids and recycled rubber in railroad infrastructure for enhanced performance." *Geosciences*, 9(1).
- Itasca (2018). "Particle flow code in three dimensions (PFC3D)." Itasca Consulting Group, Inc.
- Jiang, H., Bian, and Chen, R. (2016). "Simulating train moving loads in physical model testing of railway infrastructure and its numerical calibration." *Acta Geotechnica*, 11(2): 231-242.
- Jing, G., Wang, J., and Siahkouhi, M. (2020). "Numerical investigation of the behavior of stone ballast mixed by steel slag in ballasted railway track." *Constr Build Mater*. 262: 120015.
- Li, D., Hyslip, J., Sussmann, T. and Chrismer, S. (2015). *Railway geotechnics*, CRC Press.
- Lobo-Guerrero, S. and Vallejo, L. E. (2006). "Discrete element method analysis of railtrack ballast degradation during cyclic loading." *Granular Matter*, 8(3-4): 195-204.
- Lu, M. and McDowell, G. R. (2010). "Discrete element modelling of railway ballast under monotonic and cyclic triaxial loading." *Geotechnique*, 60(6): 459-467.
- Ngo, T., Indraratna, and Rujikiatkamjorn, C. (2017). "A study of the geogrid-subballast interface via experimental evaluation and discrete element modelling." *Granular Matter* 19(3).
- Ngo, T., Indraratna, and Rujikiatkamjorn. (2017). "Stabilization of track substructure with geoinclusions: experimental evidence and DEM simulation." *Int. J. Rail Transp.* 5(2): 63-86.
- Ngo, T., Indraratna B., and Ferreira F., 2021. Influence of synthetic inclusions on the degradation and deformation of ballast under heavy-haul cyclic loading. *International Journal of Rail Transportation*: <https://doi.org/10.1080/23248378.2021.1964390>
- O'Sullivan, C. and Cui, L. (2009). "Micromechanics of granular material response during load reversals: Combined DEM and experimental study." *Powder Technology* 193(3): 289–302.
- Ouadfel, H. and Rothenburg, L. (2001). "Stress–force–fabric relationship for assemblies of ellipsoids." *Mechanics of Materials* 33(4): 201-221.
- Priest, J. A., Powrie, W., Yang, L., and Clayton, C. R. I. (2010). "Measurements of transient ground movements below a ballasted railway line." *Geotechnique*, 60(9): 667–677.
- Qian, Y., Tutumluer, E., Mishra, D., & Kazmee, H., (2018). "Triaxial Testing and Discrete-Element Modelling of Geogrid-Stabilized Rail Ballast", *Proceedings of the Institution of Civil Engineers: Ground Improvement*, Vol. 171, Issue 4, pp. 223-231.
- Selig and Waters. (1994). *Track geotechnology and substructure management*, Thomas Telford.
- Tang, Yang, Ren, Xiao, S. (2019). "Dynamic response of soft soils in high-speed rail foundation: in situ measurements and element method model." *Can. Geotech. J.* 56(12): 1832-1848.
- Tutumluer, E, Huang, H., and Bian, X. (2009). "Research on the Behavior of Geogrids in Stabilization Applications," In *Proceedings of the Jubilee Symposium on Polymer Geogrid Reinforcement*, London, UK.
- Tutumluer, E., Huang, H. and Bian, X. (2012). "Geogrid-Aggregate Interlock Mechanism Investigated through Aggregate Imaging-Based Discrete Element Modeling Approach." *Int. J. Geomech.* 12(4): 391-398.
- Tutumluer, E., Qian, Y., Hashash, Y., Ghaboussi, J. and Davis, D. D. (2013). "Discrete element modelling of ballasted track deformation behaviour." *Int. J. Rail Transp.* 1(1-2): 57-73.
- Zhang, X., and Zhai, W. (2017). "Dynamic behavior analysis of high-speed railway ballast under moving vehicle loads using discrete element method." *Int. J. Geomech.* 17(7): 04016157.